

<sup>12</sup>J. K. Dickens, E. Eichler, and G. R. Satchler, Phys. Rev. **168**, 1355 (1968); J. K. Dickens, E. Eichler, R. J. Silva, and G. Chilosa, Oak Ridge National Laboratory Report No. ORNL-3934, 1966 (unpublished).

<sup>13</sup>W. R. Smith, University of Southern California Report No. USC 136-119, 1967 (unpublished).

<sup>14</sup>E. B. Dally, J. B. Nelson, and W. R. Smith, Phys. Rev. **152**, 1072 (1966).

<sup>15</sup>C. M. Perey and F. G. Perey, Phys. Rev. **152**, 923 (1966).

<sup>16</sup>P. Kossanyi-Demay and R. de Swiniarski, Nucl. Phys. **A104**, 577 (1968).

<sup>17</sup>F. G. Perey, Phys. Rev. **131**, 745 (1963).

<sup>18</sup>Configurations for the states of  $^{93}\text{Zr}$  are taken as given

by B. L. Cohen and O. V. Chubinsky, Phys. Rev. **131**, 2184 (1963), except for the 3.38-MeV state, here assigned as  $l \geq 2$ .

<sup>19</sup>W. Booth, S. M. Dalgiesh, R. N. Glover, R. F. Hudson, and K. C. McLean, Phys. Letters **30B**, 335 (1969).

<sup>20</sup>J. J. Kent, K. P. Lieb, and C. F. Moore, Phys. Rev. **C 1**, 337 (1970).

<sup>21</sup>T. Tamura, F. Rybicki, and W. R. Coker, to be published.

<sup>22</sup>P. J. A. Buttle and L. J. B. Goldfarb, Proc. Phys. Soc. (London) **83**, 701 (1964).

<sup>23</sup>M. Lynen, C. V. D. Malsburg, R. Santo, and R. Stock, Phys. Letters **24B**, 237 (1967).

## Gamma Rays from Thermal and Resonance Neutron Capture in $\text{Sb}^{121}$ and $\text{Sb}^{123}$ †

M. R. Bhat, R. E. Chrien, D. I. Garber, and O. A. Wasson

Brookhaven National Laboratory, Upton, New York 11973

(Received 27 March 1970)

Prompt high-energy  $\gamma$  rays resulting from neutron capture at thermal energies and in the resonances of  $\text{Sb}^{121}$  and  $\text{Sb}^{123}$  have been studied with the high flux beam reactor fast chopper using high-resolution Ge(Li) detectors. The binding energy  $B_n$  of the last neutron in  $\text{Sb}^{122}$  and  $\text{Sb}^{124}$  has been determined to be  $6807 \pm 2$  and  $6468 \pm 2$  keV, respectively. Based on prompt capture  $\gamma$ -ray data, we have assigned a spin of 4 to the 21.6-eV resonance of  $\text{Sb}^{123}$ . Energy levels populated by the neutron-capture  $\gamma$  rays are given up to an excitation energy of 2475 keV in  $\text{Sb}^{122}$  and up to 2221 keV in  $\text{Sb}^{124}$ . These data are compared with the existing  $(d, p)$  data on  $\text{Sb}^{121}$  and  $\text{Sb}^{123}$ . We have also studied the low-energy (<511 keV)  $\gamma$  rays originating in neutron capture in the different resonances. For  $\text{Sb}^{121}$ , the observed spectra are found to fall into two classes, each having its own characteristic intensity distribution depending on the spin of the capturing state. By comparing these spectra with those originating from the 6.24-eV resonance ( $3^+$ ) and the 15.4-eV resonance ( $2^+$ ), we have assigned the following spins to the resonances in  $\text{Sb}^{121}$ : 29.7 eV (3), 53.5 eV (2), 64.5 eV (3), 73.8 eV (2), 111.4 eV (2), and 126.8 eV (3). Similar, but more tentative, spin assignments are made for resonances in  $\text{Sb}^{123}$ .

The low-energy spectra have also been used to measure the half-life of the 61.6-keV isomeric state in  $\text{Sb}^{122}$  by a new method. This experimental procedure is described. The half-life of the isomeric state is found to be  $2.3 \pm 0.6 \mu\text{sec}$ .

### 1. INTRODUCTION

Antimony is made up of two isotopes,  $\text{Sb}^{121}$  and  $\text{Sb}^{123}$ , with fractional abundances of 57.25 and 42.75%, respectively. Neutron capture in these isotopes populates levels in  $\text{Sb}^{122}$  and  $\text{Sb}^{124}$  by  $\gamma$ -ray emission. Except for the  $(d, p)$  work on  $\text{Sb}^{121}$  and  $\text{Sb}^{123}$  by Hjorth,<sup>1</sup> a study<sup>2,3</sup> of some low-lying levels of  $\text{Sb}^{122}$  and  $\text{Sb}^{124}$ , and some recent resonance  $(n, \gamma)$  measurements by Ing *et al.*,<sup>4</sup> there are no data on the energy levels of  $\text{Sb}^{122}$  and  $\text{Sb}^{124}$ . In the  $(d, p)$  data mentioned above, the resolution was limited to 40 keV. Also, the zero of the energy scale, and hence the binding energy of the last neutron in these odd-odd nuclei, was not known. Hence, it seemed to be of some interest to study neutron-capture  $\gamma$  rays in antimony. Great interest has been shown in the Sn-Sb region of the periodic ta-

ble, and detailed calculations have been made using the short-range residual interactions to take account of nuclear pairing effects.<sup>5,6</sup> We hope to supplement the experimental data on nuclei in this region with the present experimental work.

### 2. EXPERIMENTAL ARRANGEMENT

Neutron-capture  $\gamma$  rays in antimony were studied using the fast chopper at the high-flux beam reactor (HFBR) with a flight path of 21.66 m and a chopper speed of 10 000 rpm. Details of the chopper installation and the on-line data recording and analyzing system have been described before.<sup>7,8</sup> The chopper was operated at 1500 rpm for recording thermal-neutron-capture events.  $\gamma$  rays originating in resonance capture were recorded with a 10-cc Ge(Li) detector at a resolution of 10 keV at 7.7

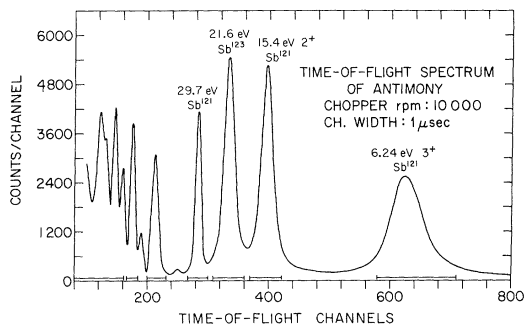


FIG. 1. Time-of-flight spectrum of Sb.

MeV. Thermal capture was mainly recorded with a 37-cc detector having a resolution of 7 keV at 7.7 MeV, except for a short run with the 10-cc detector to intercalibrate the resonance-neutron-capture  $\gamma$ -ray intensities as described below. The sample weighed 854 g, and the total running time for this experiment was 144 h.

### 3. EXPERIMENTAL RESULTS

#### A. High-Energy $\gamma$ -Ray Spectra

The time-of-flight spectrum of antimony is shown

in Fig. 1. The resonances of  $Sb^{121}$  (target spin and parity  $\frac{5}{2}^+$ ) at 6.24, 15.4, and 29.7 eV, and the 21.6-eV resonance of  $Sb^{123}$  (target spin and parity  $\frac{7}{2}^+$ ) are shown clearly resolved. Measurements of Stolovy<sup>9</sup> have given spins of  $3^+$  and  $2^+$  for the 6.24- and 15.4-eV resonances, respectively. Straight lines drawn under the resonances indicate the scan limits set on the time of flight to obtain the neutron-capture  $\gamma$  rays resulting from these resonances. Other resonances on the higher-energy side of the 29.7-eV resonances are incompletely resolved.

In Fig. 2 we show the  $\gamma$  spectra due to capture in the three resonances of  $Sb^{121}$ .<sup>10</sup> The peak marked 1 in the 15.4- and 29.7-eV resonances has been assigned to the ground-state transition in  $Sb^{122}$  and has an energy of  $6807 \pm 2$  keV obtained with the aluminum  $\gamma$  ray at 7723.8 keV as reference. This agrees quite well with the neutron binding energy of  $6804 \pm 17$  keV in  $Sb^{122}$  obtained by Damerow, Ries, and Johnson<sup>11</sup> from mass-spectroscopic data, and  $6805.5 \pm 1.0$  keV given by Rasmussen *et al.*<sup>12</sup> With this as the binding energy, the small peak marked 2 in the 6.2-eV resonance is found to populate the 62-keV  $3^+$  excited state ob-

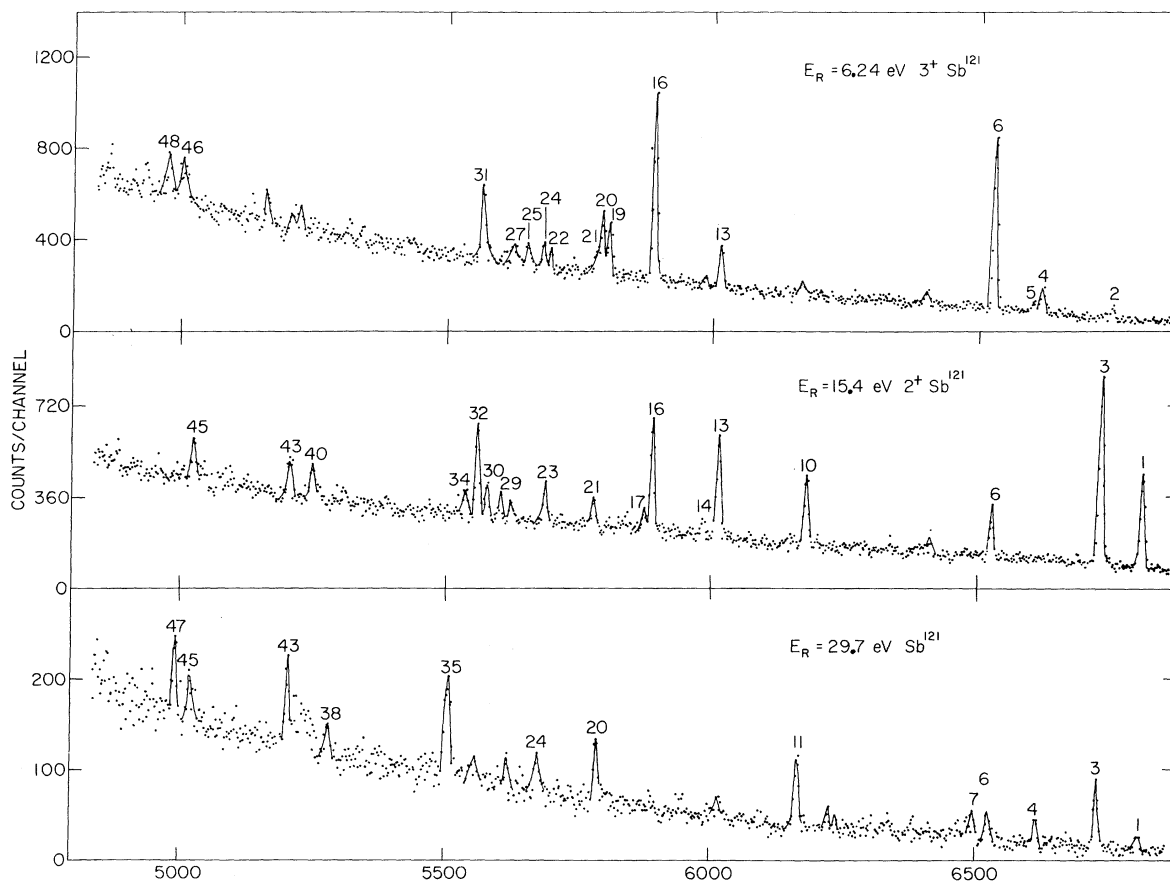
FIG. 2.  $\gamma$ -ray spectra due to capture in the three resonances of  $Sb^{121}$ .

TABLE I.  $\gamma$ -ray energies and intensities in  $\text{Sb}^{121}$  resonances.

Peak No.	$E_\gamma$ (keV)	$E_{\text{ex}}$ (keV)	Partial widths $\Gamma_{\gamma i}$ (meV)		
			6.24 eV	15.4 eV	29.7 eV
64	4331.3	2475.3	0.42±0.09	0.38±0.11	<0.2
63	4342.5	2464.1	<0.1	0.28±0.10	<0.2
62	4370.0	2436.6	0.30±0.08	<0.1	<0.2
61	4459.3	2347.3	0.35±0.08	<0.1	<0.2
60	4560.6	2246.0	<0.1	0.24±0.04	<0.2
59	4601.6	2205.0	<0.1	0.47±0.08	<0.2
58	4621.2	2185.4	0.21±0.07	<0.1	<0.2
57	4649.5	2157.1	0.40±0.08	<0.1	<0.2
56	4655.9	2150.7	<0.1	0.32±0.08	<0.2
55	4685.3	2121.3	0.62±0.06	<0.1	<0.2
54	4727.7	2078.9	0.13±0.02	<0.2	<0.2
53	4777.1	2029.5	0.36±0.04	<0.1	<0.2
52	4788.6	2018.0	0.33±0.04	<0.1	<0.2
51	4845.5	1961.1	0.15±0.06	<0.1	0.24±0.11
50	4861.6	1945.0	0.40±0.09	<0.1	<0.2
49	4927.6	1879.0	0.38±0.06	<0.1	<0.2
48	4971.2	1835.4	0.48±0.10	<0.1	<0.2
47	4990.3	1816.3	<0.1	<0.1	0.70±0.17
46	4998.3	1808.3	0.47±0.06	<0.1	<0.1
45	5019.8	1786.8	<0.1	0.57±0.09	0.62±0.19
44	5155.0	1651.6	0.40±0.06	<0.1	<0.2
43	5203.1	1603.5	0.18±0.06	0.58±0.10	0.79±0.12
42	5217.8	1588.8	0.20±0.06	<0.1	0.40±0.09
41	5235.6	1571.0	<0.1	<0.1	0.51±0.1
40	5245.3	1561.3	<0.2	0.49±0.03	0.21±0.09
39	5259.1	1547.5	<0.1	0.21±0.02	<0.1
38	5279.5	1527.1	<0.1	<0.1	0.43±0.08
37	5306.2	1500.4	<0.2	0.18±0.04	<0.2
36	5309.4	1497.2	0.13±0.05	<0.1	<0.1
35	5505.6	1301.0	<0.1	<0.1	1.46±0.14
34	5532.7	1273.9	<0.1	0.25±0.08	<0.2
33	5548.1	1258.5	<0.1	<0.1	0.20±0.05
32	5555.7	1250.9	<0.1	1.13±0.05	<0.2
31	5560.8	1245.8	0.83±0.06	<0.1	0.23±0.05
30	5573.8	1232.8	<0.1	0.38±0.07	<0.2
29	5598.8	1207.8	<0.2	0.23±0.05	<0.2
28	5616.9	1189.7	0.25±0.05	<0.1	0.24±0.06
27	5619.8	1186.8	<0.1	0.18±0.04	<0.2
26	5626.8	1179.8	0.12±0.04	<0.1	<0.2
25	5646.0	1160.6	0.28±0.03	<0.1	<0.2
24	5675.2	1131.4	0.26±0.03	<0.1	0.50±0.09
23	5683.2	1123.4	<0.1	0.43±0.06	<0.1
22	5688.3	1118.3	0.19±0.02	<0.1	<0.1
21	5774.3	1032.3	0.31±0.04	0.35±0.07	<0.2
20	5786.4	1020.2	0.64±0.05	<0.1	0.72±0.09
19	5799.8	1006.8	0.53±0.04	<0.1	<0.2
18	5802.9	1003.7	<0.1	<0.1	0.16±0.05
17	5869.0	937.6	<0.1	0.25±0.03	<0.2
16	5884.1	922.5	1.91±0.08	1.28±0.06	<0.2
15	5979.4	827.2	0.12±0.03	0.23±0.05	<0.1
14	5995.7	810.9	<0.1	<0.1	0.23±0.10
13	6008.1	798.5	0.44±0.04	1.22±0.07	<0.1
12	6015.9	790.7	<0.1	<0.1	0.27±0.13
11	6162.1	644.5	0.16±0.03	<0.1	0.68±0.06
10	6173.7	632.9	<0.1	0.89±0.05	<0.2
9	6396.5	410.1	0.20±0.04	<0.1	<0.1
8	6409.0	397.6	0.05±0.02	0.18±0.07	<0.2

TABLE I (Continued)

Peak No.	$E_\gamma$ (keV)	$E_{\text{ex}}$ (keV)	Partial widths $\Gamma_{\gamma i}$ (meV)		
			6.24 eV	15.4 eV	29.7 eV
7	6493.3	313.3	<0.1	<0.1	0.38±0.14
6	6523.1	283.5	2.05±0.10	0.46±0.06	0.22±0.07
5	6597.7	208.9	0.13±0.02	<0.1	<0.1
4	6613.2	193.4	0.32±0.03	<0.1	0.28±0.04
3	6728.4	78.2	<0.1	2.58±0.11	0.75±0.07
2	6745.0	61.6	0.24±0.03	<0.1	<0.1
1	6806.6	0.0	<0.1	1.37±0.07	0.13±0.05

served by der Mateosian and Sehgal.<sup>2</sup> Energies of other excited states in  $\text{Sb}^{122}$  populated by the  $\gamma$  rays are given in Fig. 3 up to about 1 MeV. For comparison, we show the energy levels obtained from the  $(d, p)$  data of Hjorth.<sup>1</sup> Since there was an uncertainty in the zero of the energy scale, we have arbitrarily added 27 keV to the  $(d, p)$  data to obtain the energy levels shown. However, because of the limited resolution (of the order of 40 keV) in that work, many closely spaced levels could not be resolved. Next to this is shown the data from the *Table of Isotopes*.<sup>13</sup> We assume that all the observed high-energy  $\gamma$  rays represent primary transitions, an assumption which is expected to be valid for medium and heavy nuclei.

In Table I are listed the  $\gamma$ -ray intensities observed in  $\text{Sb}^{121}$ , and their energies. Experimental errors in these energies are approximately 2 keV. These results were obtained by calibrating the  $\gamma$ -ray intensities against a thermal-neutron spectrum, as has been described in detail,<sup>14</sup> and assuming the value of (1.18 photons)/(100 neutron captures) for the intense 6523.6-keV  $\gamma$  ray as given by Rasmussen *et al.*<sup>12</sup> In Table II, we compare the intensities of some of the more intense  $\gamma$  rays against the usual Weisskopf single-particle estimates,<sup>15</sup> assuming a spacing<sup>16</sup> of  $D=10.3$  eV and also that the observed transitions are  $E1$ . The 61.6-keV excited state has been assigned a spin of  $3^+$  by der Mateosian and Sehgal.<sup>2</sup> This assignment is based on the  $E1$  character of the 61-keV transition, as indicated by comparing the intensities of the unconverted  $\gamma$  rays of this transition and the  $K$  x rays resulting from its  $K$ -shell conversion. If we accept this spin assignment, the 6745-keV  $\gamma$  ray feeding this level is an  $M1$  transition and is found to be 27 times the single-particle estimate. It has been suggested from previous experimental work<sup>17</sup> that this is a region of enhanced  $M1$  transitions perhaps corresponding to an  $M1$  giant resonance region, as suggested by Mottleson<sup>18</sup> and Bergqvist.<sup>19</sup> Hence, it is possible that a substantial fraction of the observed primary transitions

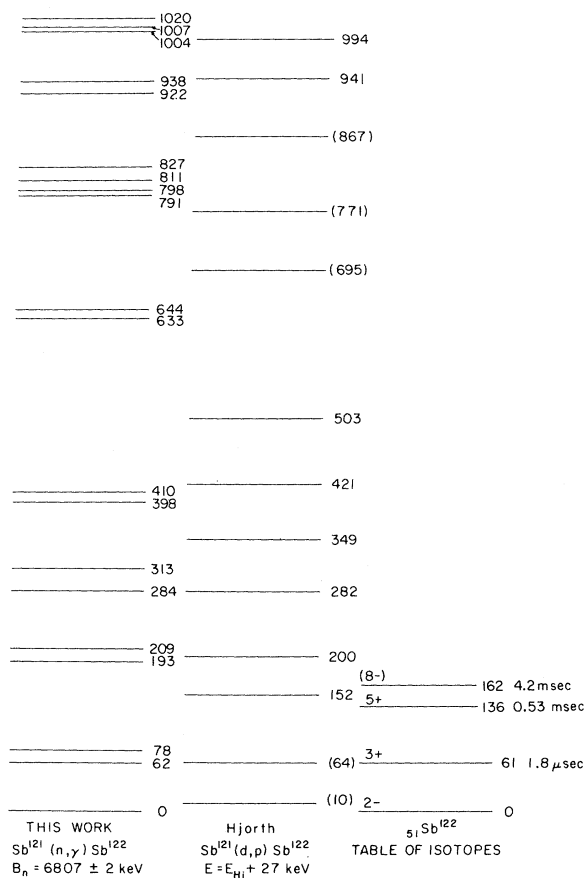


FIG. 3. Excited states in Sb<sup>122</sup>. The present experiment compared with the Hjorth (*d, p*) data and nuclear spectroscopy data.

TABLE II. Comparison of Sb  $\gamma$ -ray intensities with Weisskopf estimates.  $\Gamma_{sp}$  is defined here in terms of the Weisskopf estimate as employed by Bartholomew:

$$\Gamma_{\gamma}(E1) = 0.11 A^{2/3} (D/D_0) E_{\gamma}^3,$$

$$\Gamma_{\gamma}(M1) = 0.021 (D/D_0) E_{\gamma}^3,$$

$$D_0 = 15 \text{ MeV}.$$

Target nucleus	$E_{\gamma}$ (keV)	$\gamma$ -transition type	$\Gamma_{\gamma i}$ (meV)	$\Gamma_{\gamma i}/\Gamma_{sp}$
Sb <sup>121</sup>	6807	E1	1.37	1
	6745	M1	0.24	27
	6728	(E1)	2.58	2
	6523	(E1)	2.05	2
	6174	(E1)	0.89	1
	6008	(E1)	1.22	2
	5884	(E1)	1.92	3
	5556	(E1)	1.13	2
	5506	(E1)	1.46	2
	Sb <sup>123</sup>	6468	E1	1.77
6458		M1	0.62	40
6380		(E1)	3.46	2
6336		(E1)	1.38	1

are M1, but until further data on the spins and parities of these levels are known, no positive statement about the multipolarities can be made.

The neutron-capture spectrum of the 21.6-eV resonance of Sb<sup>123</sup> is shown in Fig. 4. In this spectrum, there is a peak at about 6500 keV, which is clearly a doublet and could be resolved into two  $\gamma$  peaks (Nos. 1 and 2) 10.5 keV apart. From nuclear spectroscopy data,<sup>3</sup> it is known that Sb<sup>124</sup> has a 93-sec isomeric state at 10-keV excitation energy. Hence, we assign these two  $\gamma$  rays as transitions, respectively, to the ground state and the 10-keV excited state of Sb<sup>124</sup>. From their energies, we

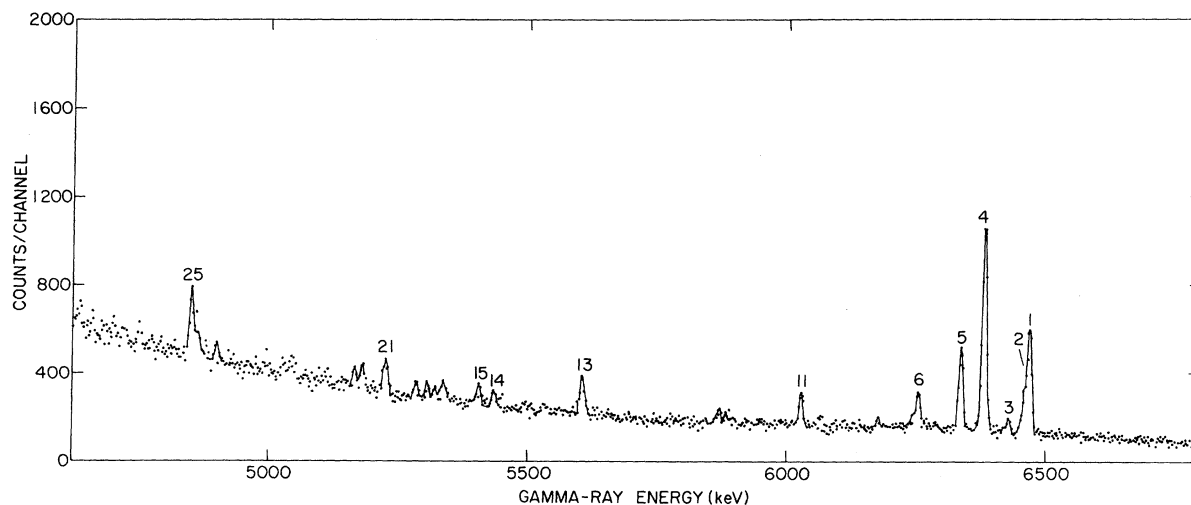


FIG. 4. Capture spectrum in the 21.6-eV resonance of Sb<sup>123</sup>.

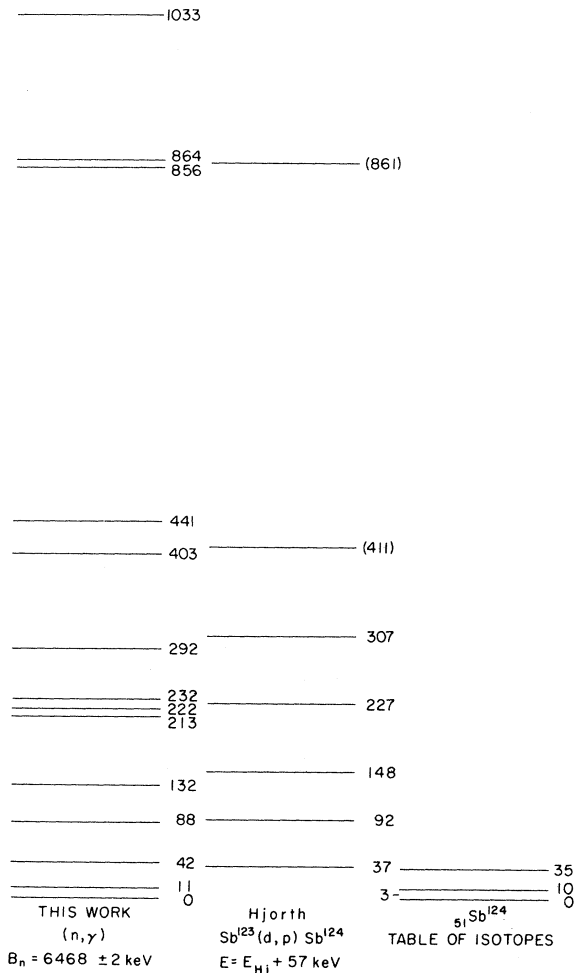


FIG. 5. Energy level diagram of  $Sb^{124}$ . The present experiment compared with the Hjorth ( $d, p$ ) and nuclear spectroscopy data.

infer that the binding energy of the last neutron is  $6468 \pm 2$  keV. This agrees quite well with the mass-spectroscopic measurements of Damerow, Ries, and Johnson,<sup>11</sup> which give a value of  $6459 \pm 10$  keV. The energy level diagram of  $Sb^{124}$  thus obtained from our data is shown in Fig. 5 up to an excitation energy of about 1 MeV along with the ( $d, p$ ) data of Hjorth and the two levels determined from low-energy nuclear spectroscopy measurements of VanHorenbeeck.<sup>3</sup> Since there was an uncertainty in the knowledge of the zero of the energy scale of the ( $d, p$ ) data, we have arbitrarily added 57 keV to the energy values of the levels as given by Hjorth. In Table III we have also listed the energies and intensities of the transitions observed in  $Sb^{123}$ , and the peak numbers correspond to those shown in Fig. 4. In Table II we give the intensities of some of the more intense  $\gamma$  transitions in this list with Weisskopf single-particle estimates, assuming that these are  $E1$  transitions. In calculating these estimates, we assume  $D = 20.7$  eV.<sup>16</sup> VanHorenbeeck<sup>3</sup> has assigned a spin of  $5^+$  to the 10-keV level in  $Sb^{124}$ , based on conversion-electron spectra, which indicated an  $M2$  transition from this 93-sec isomeric state to the 3- ground state. With this spin assignment we note that the 6458-keV  $\gamma$  ray to this state is an  $M1$  or an  $E2$  transition. If it is  $E2$ , the enhancement factor is 275. If we assume, as is more likely, that this is an  $M1$  transition, we find that the observed  $\gamma$  ray is enhanced by a factor of 40 over the single-particle estimate. This would also imply that the spin of the 21.6-eV resonance in  $Sb^{123}$  is 4.

In Fig. 6 we show the thermal-neutron-capture spectrum obtained with natural antimony. The peak numbers shown correspond to the  $\gamma$ -ray energies given in Table IV. We recorded two spectra with thermal neutrons—one with a 10-cc detec-

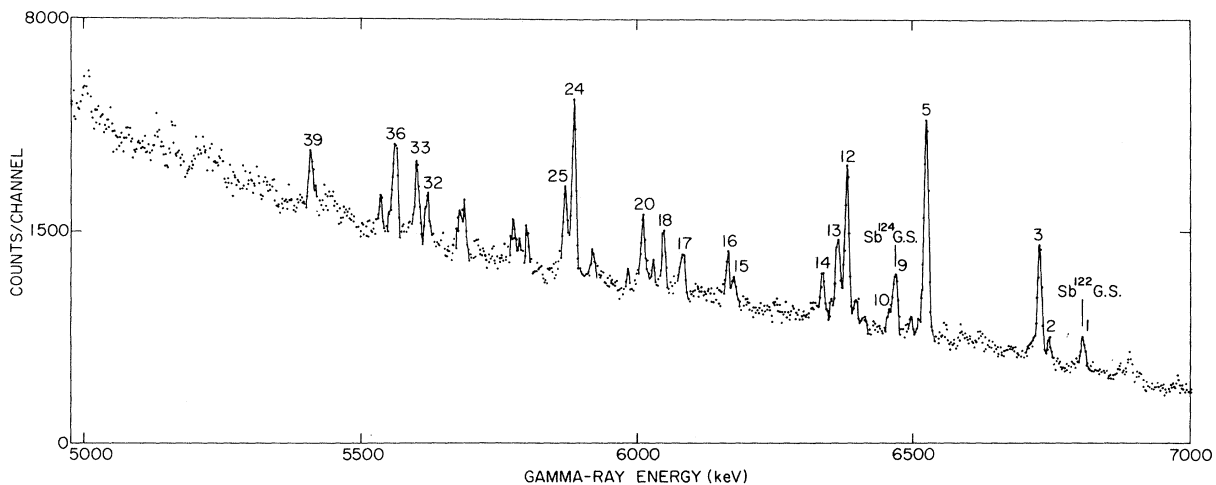


Fig. 6. Thermal spectrum of natural antimony.

TABLE III.  $\gamma$ -ray energies and intensities in the 21.6-eV resonance of  $\text{Sb}^{123}$ .

Peak No.	$E_\gamma$ (keV)	$E_{ex}$ (keV)	Partial widths		Peak No.	$E_\gamma$ (keV)	$E_{ex}$ (keV)	Partial widths	
			$\Gamma_{\gamma i}$ (meV)					$\Gamma_{\gamma i}$ (meV)	
35	4246.9	2221.2	0.25±0.04		17	5338.1	1130.0	0.40±0.09	
34	4288.3	2179.8	0.16±0.07		16	5392.4	1075.7	0.12±0.04	
33	4302.4	2165.7	0.74±0.12		15	5406.6	1061.5	0.34±0.06	
32	4417.4	2050.7	0.57±0.11		14	5435.4	1032.7	0.25±0.06	
31	4428.9	2039.2	0.60±0.12		13	5604.2	863.9	0.50±0.12	
30	4514.8	1953.3	0.46±0.11		12	5612.6	855.5	0.16±0.12	
29	4585.3	1882.8	0.39±0.12		11	6027.5	440.6	0.52±0.04	
28	4634.7	1833.4	0.54±0.10		10	6065.0	403.1	0.18±0.06	
27	4721.5	1746.6	0.39±0.07		9	6176.3	291.8	0.21±0.04	
26	4750.9	1717.2	0.42±0.07		8	6236.0	232.1	0.11±0.02	
25	4850.7	1617.4	0.99±0.12		7	6246.0	222.1	0.15±0.06	
24	4862.3	1605.8	0.56±0.09		6	6254.7	213.4	0.55±0.04	
23	5165.7	1302.4	0.37±0.06		5	6336.0	132.1	1.38±0.12	
22	5180.6	1287.5	0.50±0.08		4	6380.2	87.9	3.46±0.15	
21	5224.6	1243.5	0.72±0.08		3	6426.0	42.1	0.30±0.07	
20	5283.8	1184.3	0.27±0.05		2	6457.6	10.5	0.62±0.07	
19	5307.1	1161.0	0.22±0.04		1	6468.1	0.0	1.77±0.09	
18	5321.0	1147.1	0.14±0.03						

tor to calibrate the intensity of the resonance-neutron-capture  $\gamma$  rays and the other with a 37-cc detector. The spectrum shown corresponds to the latter. A list of the  $\gamma$  rays observed is shown in Table IV along with those observed by Rasmussen *et al.*<sup>12</sup> For the sake of comparison, we have normalized our intensities to the most intense  $\gamma$  ray at 6523.6 keV, and the normalized intensities are given along with Rasmussen's values. The agreement in energy values is very good; in intensities it is fair.

#### B. Low-Energy $\gamma$ -Ray Spectra

In addition to the prompt high-energy  $\gamma$ -ray spectra, we have also recorded low-energy ( $\leq 0.511$  MeV)  $\gamma$  rays originating in neutron capture in the resonances of  $\text{Sb}^{121}$  and  $\text{Sb}^{123}$ . Since these  $\gamma$  rays originate from states which are fed by prompt  $\gamma$  rays from the compound-nucleus resonances, we can expect the wide fluctuations in the intensities of these  $\gamma$  rays to be smoothed out in averaging over the many cascades feeding the low-lying levels. This is indeed found to be true and in the following sections we will describe the use of these  $\gamma$  rays to: (i) assign spins to the capturing states, and (ii) describe a novel method of determining the half-life of a low-lying isomeric state at 61 keV in  $\text{Sb}^{122}$ .

##### i. Spin Assignment of S-Wave Neutron Resonances from Low-Energy $\gamma$ Rays

In neutron capture, the compound nucleus formed decays by emitting one or more  $\gamma$  rays. The average number emitted per capture is found experi-

mentally to be between 3 and 5. Such a  $\gamma$  cascade populates the different energy levels of the compound nucleus lying between the neutron binding energy and the ground state. The relative probabilities for populating those states could be expected to depend on their spins relative to the spin of the capturing state. Some of the early measurements of such probabilities were made in terms of the "isomeric ratios"—and differences in these ratios were indeed found to depend on the spins of the neutron resonances. A summary of this early experimental work may be found in the article by Kinsey.<sup>20</sup> With improvements in experimental technique, measurements were made on the low-energy  $\gamma$  spectra from resonant capture, so that the relative probabilities for populating all the low-lying nuclear states in addition to the isomeric states could be determined. Draper, Fenstermacher, and Schultz<sup>21</sup> measured the  $\gamma$  spectra from the 1.46-, 3.86-, and 9.10-eV resonances of  $\text{In}^{115}$  using a NaI(Tl) detector and found that the spectra differed with respect to the relative intensities of the 67-, 98-, 188-, and 280-keV  $\gamma$  rays. This was followed by the measurements of Fenstermacher, Draper, and Bockelman<sup>22</sup> on  $\text{Er}^{167}$  and  $\text{Hf}^{177}$ . These are even-odd nuclei which form an even-even compound-nuclear system by neutron capture. They measured the relative intensities of the  $\gamma$  rays corresponding to transitions between the  $6^+$ ,  $4^+$ ,  $2^+$ , and  $0^+$  members of the rotational band. The measured ratios were interpreted in terms of a simple  $\gamma$ -cascade model by Huizenga and Vandenbosch,<sup>23</sup> and they were able to assign some resonance spins for these nuclei. In constructing such a model,

TABLE IV. Energies and intensities of the thermal-neutron-capture  $\gamma$  rays in antimony.

Peak No.	This experiment		Rasmussen <i>et al.</i>	
	$E_\gamma$ (keV)	$I_\gamma$	$E_\gamma$ (keV)	$I_\gamma$
59	4565.0	0.17	4567.0	0.14
			4586.7	0.04
58	4605.0	0.15	4603.0	0.12
57	4624.7	0.14	4623.8	0.07
56	4642.0	0.20	4648.7	0.11
55	4659.2	0.25		
54	4691.0	0.31	4662.1	0.06
			4689.8	0.22
			4761.4	0.05
53	4734.3	0.09		
52	4779.5	0.11	4780.7	0.09
51	4820.4	0.17	4819.5	0.19
50	4905.1	0.20	4906.5	0.08
49	4932.0	0.20	4930.3	0.15
48	4998.2	0.18		
			5004.9	0.26
47	5007.5	0.21		
			5046.3	0.07
			5077.4	0.06
46	5129.3	0.16	5127.0	0.20
45	5159.1	0.16	5158.8	0.08
44	5202.2	0.10		
43	5214.4	0.20		
42	5223.9	0.18		
41	5245.5	0.18	5246.1	0.09
40	5311.4	0.15	5312.3	0.12
			5337.2	0.09
39	5409.1	0.27	5408.4	0.28
			5433.4	0.06
			5450.7	0.09
			5468.0	0.06
			5519.3	0.05
			5537.0	0.06
38	5535.6	0.21		
37	5554.7	0.18		
36	5563.4	0.57	5562.9	0.65
35	5577.2	0.06		
34	5589.6	0.05		
33	5602.2	0.47	5600.8	0.29
32	5621.3	0.32	5619.8	0.18
31	5647.0	0.09		
30	5676.2	0.16		
29	5686.8	0.33	5684.3	0.33
28	5776.8	0.22		
27	5788.6	0.12		
26	5802.1	0.19	5801.0	0.05
25	5870.4	0.49	5868.6	0.23
24	5886.2	0.88	5886.2	0.60
23	5920.6	0.09		
22	5938.1	0.05	5933.3	0.05
21	5983.6	0.06		
20	6011.3	0.45	6009.4	0.26
19	6028.7	0.13		
18	6048.6	0.33	6048.9	0.21
17	6082.8	0.15	6082.9	0.29
16	6165.0	0.22	6165.0	0.09
15	6176.2	0.06		
14	6336.0	0.20	6335.6	0.22

TABLE IV (Continued)

Peak No.	This experiment		Rasmussen <i>et al.</i>	
	$E_\gamma$ (keV)	$I_\gamma$	$E_\gamma$ (keV)	$I_\gamma$
13	6364.8	0.57	6363.8	0.20
12	6380.5	0.88	6380.1	0.52
11	6411.8	0.07	6409.0	0.06
10	6457.1	0.16		
9	6468.1	0.44	6468.1	0.44
8	6494.6	0.12	6498.2	0.08
7	6509.5	0.07		
6	6517.7	0.27		
5	6524.7	1.18	6523.6	1.18
4	6716.8	0.13		
3	6728.9	0.72	6728.0	0.80
2	6745.6	0.11		
1	6806.6	0.16	6805.5	0.20

these authors noted the fact that relative intensities of the low-energy  $\gamma$  rays could be expected to depend on: (1) the spin of the neutron resonances, (2) the number of steps in the  $\gamma$  cascade, (3) multiplicity of the transition at each step, and (4) the spins of the different states involved in the cascade. In their calculations, only dipole transitions were assumed for simplicity. Subsequently, the cascade model has been refined by Pönitz<sup>24</sup> to include mixing of quadrupole transitions and energy-dependent factors in calculating the transition probabilities. Similar calculations have also been made by Sperber and Mandler.<sup>25</sup> Recently, there have been improved measurements of this type using the Ge(Li) detector with its high resolution, and measurements on the even-odd target nuclei Er<sup>167</sup> and Os<sup>187, 189</sup> have been reported by Wetzel and Thomas.<sup>26</sup> They have measured the transitions between the members of the rotational band of the even-even nuclei Er<sup>168</sup>, Os<sup>188, 190</sup> resulting from neutron capture and have assigned some resonance spins.

Low-energy  $\gamma$  spectra from the nine resonances in Sb<sup>121</sup> from 6.24 to 126.6 eV have been measured using a Ge(Li) detector and a flight path of 21.66 and 48.8 m at the HFBR fast chopper. The spectra show a number of prominent  $\gamma$  rays, most of them at energies less than 0.5 MeV. An examination of the relative intensities of the  $\gamma$  rays indicates that the spectra fall into two groups with respect to the intensities of the 121.2- and 114.5-keV  $\gamma$  rays. In Fig. 7 we show the spectra from the 6.24- and 15.4-eV resonances characteristic of each group. The spins of these resonances were measured by Stolovy<sup>9</sup> using a polarized neutron beam and a polarized target. The ratio of the 121.2- to the 114.5-keV  $\gamma$  peak is about 2.5 for the spin-2 resonance as compared with a value of about 1.0 for the spin-3 resonance. Some of the other  $\gamma$  rays do show a

variation of intensity from resonance to resonance, but these variations are not as marked as in the case of the two  $\gamma$  rays mentioned. The observed ratios for the nine resonances are shown in Fig. 8 with the experimental errors. There are two experimental values for the 15.4- and 29.7-eV resonances which correspond to two different sample thicknesses. It is evident that this ratio falls into two groups, and we can assign spins to these resonances to be the same as those determined directly for the 6.24- and 15.4-eV resonances, respectively. Since there are no data on the spins of the nuclear levels in  $\text{Sb}^{122}$  depopulated by these  $\gamma$  rays, it is not possible to check whether the observed ratios are consistent with a  $\gamma$ -cascade model, and any such calculations could be done only with more detailed data on the level scheme of  $\text{Sb}^{122}$ . In Fig. 8, the 89.6-eV resonance has been shown to be a closely spaced doublet,<sup>16</sup> and we are not able to resolve these. Similarly, we cannot resolve the 126.6- and 131.9-eV resonances, and we have assigned spin 3 to the 126.8-eV resonance, as it is much stronger than its companion at 131.9 eV.

Similar measurements were made on the 21.6-, 50.5-, 76.7-, and 105.0-eV resonances in  $\text{Sb}^{123}$ . The observed spectrum of the first resonance falls into a group by itself with which the spectra from the other three form a second group. Spectra from the 21.4- and 50.5-eV resonances, characteristic of each group, are shown in Fig. 9. From the observed high-energy  $\gamma$  transitions we are able to assign a spin of  $4^+$  to the 21.4-eV resonance (see Sec. 3 A). If the systematic differences in the intensities of the low-energy transitions can be validly related to capturing-state spins, then we may

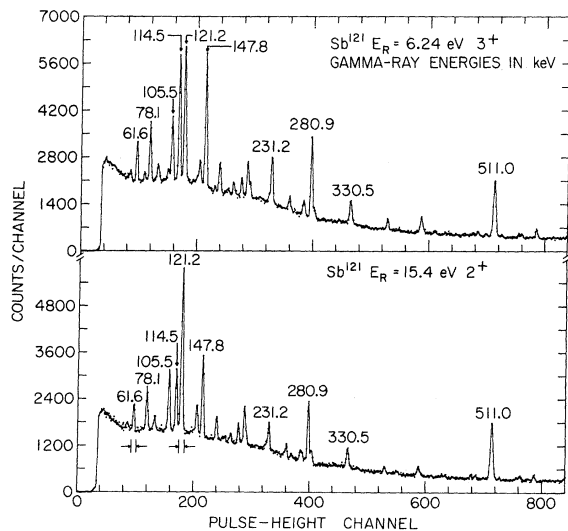


FIG. 7. Low-energy  $\gamma$  spectra from the 6.24- and 15.4-eV resonances in  $\text{Sb}^{121}$ .

assign a spin of 3 to the 50.5-, 76.7-, and 105-eV resonances.

ii. *Determination of the Half-Life of an Isomeric State Fed by Neutron Capture*

As has been described before,<sup>8</sup> each event corresponding to the emission of a  $\gamma$  ray of a particular pulse height and originating from capture by a neutron with a definite time of flight is tagged by these two parameters and is stored on magnetic tape. It is possible to set definite limits for the time-of-flight parameter and to determine all the  $\gamma$  rays originating from capture by neutrons in this time-of-flight range. This is what was done in obtaining the spectra reproduced in Figs. 2 and 4. On the other hand, we can also set specific limits on the pulse-height parameter and obtain the neutron time-of-flight spectrum corresponding to these limits. We can now ask what sort of time-of-flight spectrum we can expect to obtain if the scan limits correspond to a  $\gamma$  peak involving the decay of a state with a half-life comparable to or larger than one channel in the time-of-flight spectrum. This is shown in Fig. 10. Here we have drawn a response function  $P(t)$  (here assumed to be Gaussian) centered at channel 50 (the  $x$  axis gives time-of-flight channels in  $\mu\text{sec}$ ). One can think of this as representing a resonance in the time-of-flight spectrum if the scan limits correspond to a prompt  $\gamma$  ray. The rest of the curves are obtained by convoluting the curve  $P(t)$  by a kernel  $K(T-t)$  which is given by

$$K(T-t) = (1/\tau) e^{-(T-t)/\tau} \quad \text{for } T \geq t, \\ = 0 \quad \text{for } T < t,$$

and  $\tau$  = decay constant. These curves indicate the modified resonance peaks to be expected in the case where the  $\gamma$  ray under consideration corresponds to an isomeric transition with a half-life

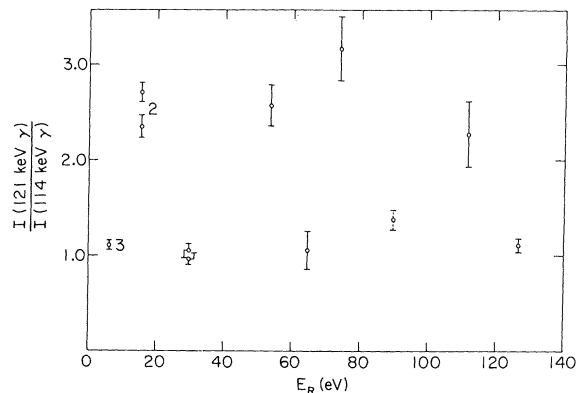


FIG. 8. Ratio of the 121.2- and 114.5-keV  $\gamma$  rays in  $\text{Sb}^{121}$  resonances.



$\geq 1 \mu\text{sec}$ . We note that this is similar to the analysis that is involved in standard delayed-coincidence measurements.<sup>27</sup> This well-known analysis indicates that (a) for short half-lives the centroid of the "delayed" curve is shifted with respect to the centroid of the "prompt" curve by an amount equal to  $\tau$ , and (b) for very large half-lives one could expect to determine the half-life from the slope of the delayed curve. This is indeed found to be true experimentally.

Before discussing the experimental details of this method and the method of extracting the half-life from the experimental data, we would like to list some of the advantages of this method. Since we can follow the decay of an excited state originating in a specific resonance, (a) a particular isotope may be isolated in a natural sample, (b) background from impurity  $\gamma$  rays are largely eliminated, and (c) isotopes with low thermal cross sections, but large resonance cross sections, may be studied.

Figure 11 shows a time-of-flight spectrum at the 15.4-eV resonance corresponding to the 121.2-keV  $\gamma$  ray in  $\text{Sb}^{121}$  as a continuous curve. This is one of the several low-energy  $\gamma$  rays in  $\text{Sb}^{121}$  which depopulate a low-lying state with a half-life very short compared with the width of one channel in the time-of-flight spectrum. Even if the actual half-life of the nuclear state is not known, it is easy to identify such a "prompt"  $\gamma$  ray. This is done by comparing the time-of-flight spectrum obtained for that transition with the time-of-flight spectrum corresponding to high-energy, or primary, capture  $\gamma$  rays. If the resonance peaks in the two spectra coincide and the resonance does not show a "tail" on its low-energy side, then the

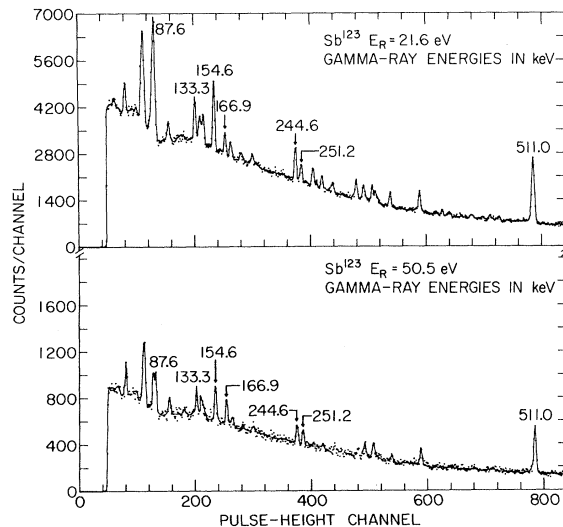


FIG. 9. Low-energy  $\gamma$  spectra from the 21.4- and 50.5-eV resonances in  $\text{Sb}^{123}$ .

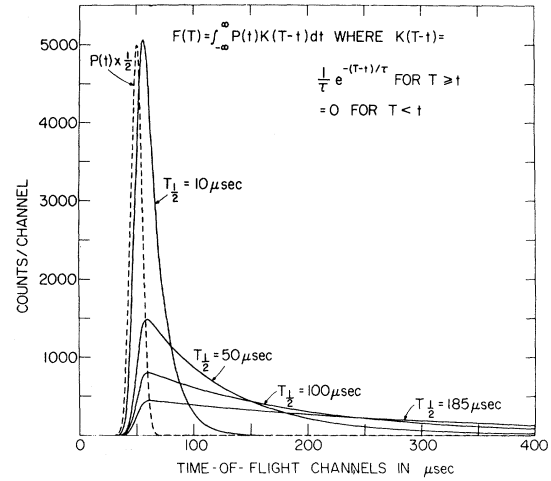


FIG. 10. Delayed curves for isomeric states of different half-lives. The ordinates of the unconvoluted curve,  $P(t)$ , have been multiplied by  $\frac{1}{2}$  for convenience.

low-energy  $\gamma$  ray can be considered as "prompt." If, on the other hand, the resonance peak in the scan of the low-energy  $\gamma$  ray is displaced with respect to the prompt spectrum and shows a "tail" on its low-energy side, then such a  $\gamma$  ray depopulates an isomeric state with a half-life comparable to or greater than a channel within the time-of-flight spectrum.

A complication arises if the sample is thick so that appreciable absorption of the neutron beam or the  $\gamma$  ray results. The effects of self-absorption are such as to introduce a distortion in the shape of the time-of-flight curve, and this distortion is dependent on the  $\gamma$ -ray energy. The effects of self-absorption distortion can be minimized by using a comparison with a prompt  $\gamma$  ray of nearly the same energy.

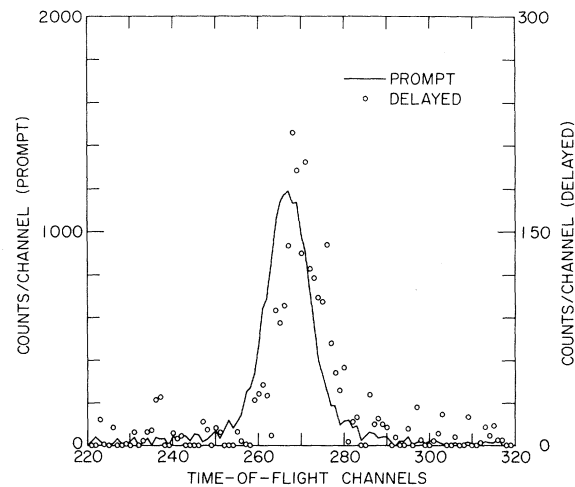


FIG. 11. Prompt and delayed curves for the 15.4-eV resonance of  $\text{Sb}^{121}$ .

Having chosen one such "prompt"  $\gamma$  ray, time-of-flight spectra are obtained corresponding to scan limits on the  $\gamma$ -ray peak, as well as the background on either side of it. The suitably normalized background spectrum is subtracted, and the result is a net "prompt" time-of-flight spectrum as shown in Fig. 11. Similarly, we obtain the net time-of-flight spectrum corresponding to the 61.6-keV  $\gamma$  ray. This is shown in Fig. 11 as dots. It is seen from Fig. 11 that the centroid of the "delayed" spectrum is shifted with respect to that of the "prompt" spectrum. In these spectra, we choose the prominent and isolated resonance at 15.4 eV to determine the half-life of the isomeric state. A base line corresponding to the smooth background region on either side of the resonance is drawn, and the "delayed" spectrum is normalized to have the same area under this resonance as the "prompt" spectrum. This is done in order to be able to compare the shapes of the resonance in the prompt and delayed spectra and since the area under the resonance is invariant under the convolution given by  $K(T-t)$ . A least-squares program has been written which compares the "delayed" spectrum with that obtained from convoluting the "prompt" spectrum with different values of  $\tau$  until a best fit is obtained. The result of such an analysis gives a half-life of  $2.3 \pm 0.6$   $\mu$ sec for the 61-keV state, which is in good agreement with a value of  $1.8 \pm 0.2$   $\mu$ sec obtained by der Mateosian and Sehgal<sup>2</sup> using conventional methods.

#### 4. DISCUSSION

The data of Table II imply the presence of anomalously strong  $M1$  transitions in the Sb isotopes. Bergqvist has suggested that such anomalously strong transitions can be associated with a simple

spin-flip transition across the spin-orbit splitting associated with the nuclear shell model. These transitions would correspond, in the continuum region, to transitions of the type  $h^{9/2} - h^{11/2}$  or  $g^{7/2} - g^{9/2}$ .

It has been pointed out by Bollinger,<sup>28</sup> however, that  $M1$  transitions observed after thermal and epithermal capture seem to be about an order of magnitude stronger than the Weisskopf estimate, in the region for  $A > 100$ . He suggests that in many nuclides  $M1$  and  $E1$  transitions are, in fact, of comparable magnitude, and gives the relation

$$\Gamma(E1)/\Gamma(M1) \approx 1.7(E_2/7)^2(A/100)^{8/3},$$

$$\approx 2.55 \text{ Sb}^{122, 124} \text{ at } 6.5 \text{ MeV.}$$

This is derived by extrapolating the giant dipole resonance to low energies, as suggested by Axel.<sup>29</sup>

There is, unfortunately, no definitive way to test this prediction in the present experiment, since few of the final-state spins are known. At best, we can compare the transitions with the ground and first excited states of Sb<sup>122</sup> and Sb<sup>124</sup> (three resonances in Sb<sup>121</sup> and one resonance in Sb<sup>123</sup>). Forming the ratio  $\Gamma(E1)/\Gamma(M1)$  over these eight transitions we get:

$$\Gamma(E1)/\Gamma(M1) \approx 4.4.$$

This, within the limited sample statistics, is not inconsistent with Bollinger's estimate, although it is a factor of 2 larger. There is, therefore, no firm evidence for any special enhancement of  $M1$  transition strength in the antimony isotopes because of a spin-flip mechanism.

A corollary of these considerations is that several of the transitions labeled  $E1$  in Table IV may be  $M1$ . It should be noted, however, that the two transitions known with reasonable certainty to be  $M1$  are in fact the weakest members of the group.

†Work supported by the U. S. Atomic Energy Commission.

<sup>1</sup>S. A. Hjorth, Arkiv Fysik **33**, 183 (1966).

<sup>2</sup>E. der Mateosian and M. L. Sehgal, Phys. Rev. **125**, 1615 (1961); **129**, 2195 (1963).

<sup>3</sup>J. VanHorenbeeck, Nucl. Phys. **37**, 90 (1962).

<sup>4</sup>H. Ing, A. Kukoe, J. D. King, and H. W. Taylor, Nucl. Phys. **A137**, 561 (1969).

<sup>5</sup>L. Kisslinger and R. Sorenson, Kgl. Danske Videnskab. Selskab, Mat.-Fys. Medd. **32**, No. 9 (1960).

<sup>6</sup>L. Kisslinger and R. Sorenson, Rev. Mod. Phys. **35**, 853 (1963).

<sup>7</sup>R. E. Chrien and M. Reich, Nucl. Instr. Methods **53**, 93 (1967).

<sup>8</sup>M. R. Bhat, B. R. Borrill, R. E. Chrien, S. Rankowitz, B. Souček, and O. A. Wasson, Nucl. Instr. Methods **53**, 108 (1967).

<sup>9</sup>A. Stolovy, Phys. Rev. **155**, 1330 (1967).

<sup>10</sup>The  $x$  axis gives the energy of the  $\gamma$  rays in keV, and the peak numbers correspond to the  $\gamma$  rays given in Table I.

<sup>11</sup>R. A. Damerow, R. R. Ries and W. H. Johnson, Jr., Phys. Rev. **132**, 1673 (1963).

<sup>12</sup>N. C. Rasmussen, V. J. Orphan, Y. Hukai, and T. Inouye, Nucl. Data **A5**, 61 (1968).

<sup>13</sup>C. M. Lederer, J. M. Hollander, and I. Perlman, *Table of Isotopes*, (John Wiley & Sons, Inc., New York, 1967).

<sup>14</sup>M. R. Bhat, R. E. Chrien, O. A. Wasson, M. Beer, and M. A. Lone, Phys. Rev. **166**, 1111 (1968).

<sup>15</sup>G. A. Bartholomew, Ann. Rev. Nucl. Sci. **11**, 259 (1961).

<sup>16</sup>G. P. Muradyan, Yu. V. Adamchuk, and Yu. G. Shchepkin, Soviet J. Nucl. Phys. **8**, 495 (1969).

<sup>17</sup>J. A. Harvey, G. G. Slaughter, J. R. Bird, and G. T. Chapman, Argonne National Laboratory Report No. ANL 6797, 1963 (unpublished), p. 230.

<sup>18</sup>B. R. Mottelson, in *Proceedings of the International Conference on Nuclear Structure, 1960, Queen's University, Kingston, Ontario*, edited by D. A. Bromley and E. W. Vogt (University of Toronto Press, 1960), p. 525.

<sup>19</sup>I. Bergqvist, B. Lundberg, and N. Starfelt, Argonne National Laboratory Report No. ANL 6797, 1963 (unpublished), p. 220.

<sup>20</sup>B. B. Kinsey, in *Encyclopedia of Physics*, edited by S. Flugge (Springer-Verlag, Berlin, Germany, 1957), Vol. XL, p. 302.

<sup>21</sup>J. E. Draper, C. Fenstermacher, and H. L. Schultz, *Phys. Rev.* **111**, 906 (1958).

<sup>22</sup>C. A. Fenstermacher, J. E. Draper, and C. K. Bockel-

man, *Nucl. Phys.* **10**, 386 (1959).

<sup>23</sup>J. R. Huizenga and R. Vandenbosch, *Phys. Rev.* **120**, 1305 (1960).

<sup>24</sup>W. P. Pönitz, *Z. Physik* **197**, 262 (1966).

<sup>25</sup>D. Sperber and J. W. Mandler, *Nucl. Phys.* **A113**, 689 (1968).

<sup>26</sup>K. J. Wetzel and G. E. Thomas, *Phys. Rev. C* **1**, 1501 (1970).

<sup>27</sup>R. E. Bell, in *Alpha-, Beta-, and Gamma-Ray Spectroscopy*, edited by K. Sieghahn (North-Holland Publishing Company, Amsterdam, The Netherlands, 1965), Vol. 2, p. 905.

<sup>28</sup>L. M. Bollinger, in *International Symposium on Nuclear Structure, Dubna, 1968* (International Atomic Energy Agency, Vienna, Austria, 1969), p. 317.

<sup>29</sup>P. Axel, *Phys. Rev.* **126**, 671 (1962).

## $\gamma$ -Vibrational and Ground-State Rotational-Band Mixing in <sup>238</sup>Pu

J. M. Palms, R. E. Wood, and P. Venugopala Rao

*Emory University, Atlanta, Georgia 30322*

(Received 26 November 1969; revised manuscript received 29 June 1970)

The intensities of the high-energy  $\gamma$  rays in the 2.1-day decay of <sup>238</sup>Np to <sup>238</sup>Pu are measured using a high-resolution Ge(Li) detector (full width at half maximum of 1.7 keV at 1333 keV). The branching ratios for the transitions from the  $\gamma$ -vibrational band are found to be consistent with values of  $(26.5 \pm 7.8) \times 10^{-3}$  for  $z$ , the band-mixing parameter for the ground-state rotational and  $\gamma$ -vibrational bands, and  $\approx -7 \times 10^{-3}$  for  $z_{\beta\gamma}$ , the parameter for the mixing of  $\beta$ - and  $\gamma$ -vibrational bands.

### I. INTRODUCTION

It is now well established that the branching ratios for the  $E2$  transitions from  $\gamma$ -vibrational bands to ground-state bands indicate a small mixing of these bands.<sup>1</sup> The rotational-vibrational interaction is usually characterized by the coupling parameter  $z$ .<sup>1,2</sup> A single value of  $z$  is expected to explain all the observed intensities of the transitions between the two bands in a nucleus. Considerable work has been done in support of such a description in the case of deformed nuclei of the rare-earth region,<sup>3-11</sup> as well as heavy deformed nuclei.<sup>12-17</sup> The strong excitation of two  $K=2$  vibrational levels at 1030 keV ( $2^+$ ) and 1071 keV ( $3^+$ ) in <sup>238</sup>Pu was well established by previous work.<sup>17-22</sup> Borggreen, Nielson, and Nordby<sup>17</sup> determined the branching ratios for the transitions deexciting these two levels from conversion-electron intensities assuming a theoretical  $\alpha_K$  for pure  $E2$  transitions. They found an average value of  $z \approx 0.025$ . In the present work the relative  $\gamma$ -ray intensities are measured using a high-resolution Ge(Li) detector with calibrated relative efficiency in order

to study the deexcitation of  $2^+$  and  $3^+$   $\gamma$ -vibrational states.

### II. EXPERIMENTAL PROCEDURE

A few  $\mu\text{g}$  of <sup>238</sup>Np were irradiated in the thermal-neutron beam from the Lockheed reactor. The  $\gamma$ -ray spectra were measured with a high-resolution (full width at half maximum of 1.7 keV at 1333 keV) Ge(Li) photon spectrometer. The detector and electronic circuitry have been discussed elsewhere.<sup>23,24</sup> The photopeak efficiency calibration of the detector was made using International Atomic Energy Agency calibrated sources.

### III. RESULTS

A typical  $\gamma$ -ray spectrum of the high-energy region is shown in Fig. 1. The decay of each of the photopeaks was followed over several half-lives. The unidentified  $\gamma$  rays in the spectrum did not belong to the decay of <sup>238</sup>Np. The closely spaced doublet of 1027.4- and 1029.9-keV  $\gamma$  rays is clearly resolved. The energies and relative intensities of the  $\gamma$  rays measured in the present experiment are presented in Table I.  $\gamma$  rays at 990 and 1034 keV corresponding to transitions from a level at 1034